Three-Dimensional Structure/Hydrophobicity of Latarcins Specifies Their Mode of Membrane Activity[†,‡]

Peter V. Dubovskii,* Pavel E. Volynsky, Anton A. Polyansky, Dmitry V. Karpunin, Vladimir V. Chupin, Roman G. Efremov, and Alexander S. Arseniev

Shemyakin-Ovchinnikov Institute of Bioorganic Chemistry, 16/10 Miklukho-Maklaya Str., Moscow 117997, Russia

Received November 3, 2007; Revised Manuscript Received January 28, 2008

ABSTRACT: Latarcins, linear peptides from the *Lachesana tarabaevi* spider venom, exhibit a broad-spectrum antimicrobial activity, likely acting on the bacterial cytoplasmic membrane. We study their spatial structures and interaction with model membranes by a combination of experimental and theoretical methods to reveal the structure−activity relationship. In this work, a 26 amino acid peptide, Ltc1, was investigated. Its spatial structure in detergent micelles was determined by ^{1}H nuclear magnetic resonance (NMR) and refined by Monte Carlo simulations in an implicit water−octanol slab. The Ltc1 molecule was found to form a straight uninterrupted amphiphilic helix comprising 8–23 residues. A dye-leakage fluorescent assay and ^{31}P NMR spectroscopy established that the peptide does not induce the release of fluorescent marker nor deteriorate the bilayer structure of the membranes. The voltage-clamp technique showed that Ltc1 induces the current fluctuations through planar membranes when the sign of the applied potential coincides with the one across the bacterial inner membrane. This implies that Ltc1 acts on the membranes via a specific mechanism, which is different from the carpet mode demonstrated by another latarcin, Ltc2a, featuring a helix−hinge−helix structure with a hydrophobicity gradient along the peptide chain. In contrast, the hydrophobic surface of the Ltc1 helix is narrow-shaped and extends with no gradient along the axis. We have also disclosed a number of peptides, structurally homologous to Ltc1 and exhibiting similar membrane activity. This indicates that the hydrophobic pattern of the Ltc1 helix and related antimicrobial peptides specifies their activity mechanism. The latter assumes the formation of variable-sized lesions, which depend upon the potential across the membrane.

An increasing antibiotic resistance requires the development of novel antibacterial drugs (*1, 2*). Linear antimicrobial peptides (L-AMPs)[1] belong to relatively simple natural host defense agents, which can be used as a template for the molecular design of effective therapeutics (*1*). According to a number of biophysical studies, these peptides are usually unordered in aqueous solution, whereas in the membrane environment, they form amphipathic helices (*3–5*). The following properties are often considered as the determinants of the L-AMP activity: amphiphilicity, the length and flexibility of the peptide helix, the spatial distribution of positive charges, and the hydrophobicity gradient along the helical axis (*2, 6*). Certain variations in these parameters can increase the peptide activity and/or selectivity toward different cell types (*7, 8*). However, the relationship between the alteration of the peptide sequence and its activity is very complicated (*9–11*). Thus, only the knowledge of the mechanism, by which the peptide molecule is acting on the cell membrane, may provide a rationale for the design of the analogues with predefined properties. Unfortunately, the individual contributions of the aforementioned factors to the L-AMP mechanism are still poorly understood. One of the possible ways to solve this task is to analyze natural peptides featuring biomolecular diversity.

Venom animals excreting a wide spectrum of L-AMP make use of different host defense strategies. The first one is to produce "universal killers", such as melittin, which is effective against many types of cells (*12*). Another strategy is to express an array of structurally similar peptides having a high cytolytic activity against cells of different origin. As a result, the venom would damage virtually any cell type (*13*). The members of such a set of L-AMP often differ in only few structural characteristics. Therefore, a detailed study

[†] This work was supported by the Russian Federation (RF) Federal Agency for Science and Innovations (Grants 4728.2006.4 and MK-5657.2006.4) and the Russian Foundation for Basic Research, project numbers 06-04-49588, 07-04-01514, and 07-04-00910.

[‡] NMR constraints and derived atomic coordinates of the peptide in detergent micelles (20 models) have been deposited in the Protein Data Bank (accession code 2PCO).

* To whom correspondence should be addressed. Telephone: (495) 335-2733. Fax: (495) 330-5565. E-mail: peter@nmr.ru.

[1] Abbreviations: 2D, two dimensional; 3D, three dimensional; AMP, antimicrobial peptide; L-AMP, linear antimicrobial peptide; CBF, carboxyfluorescein; CD, circular dichroism; CSA, chemical-shift anisotropy; CSI, chemical-shift index; DOPE, dioleoylphosphatidylethanolamine; DOPG, dioleoylphosphatidylglycerol; Ltc1, latarcin 1, spider-derived peptide with the sequence SMWSGMWRRKLKKLRNALKKKLKGEK; Ltc2a, latarcin 2a, the peptide with the sequence GLFGKLIKKFGRKAISYAVKKARGKH; L/P, lipid/protein molar ratio; MC, Monte Carlo; MHP, molecular hydrophobicity potential; LUV, large unilamellar vesicle; NMR, nuclear magnetic resonance; NOE, nuclear Overhauser effect; NOESY, 2D NOE spectroscopy; PE, phosphatidylethanolamine; PG, phosphatidylglycerol; SAR, structure−activity relationship; SDS, sodium dodecyl sulfate; SDS-d_{25}, deuterated sodium dodecyl sulfate; TFE, trifluoroethanol; TOCSY, 2D total correlation spectroscopy; ppm, parts per million.

10.1021/bi702203w CCC: $40.75
Published on Web 02/23/2008

of these peptides would provide an insight into the molecular determinants of their biological functions. One of the effective ways is to study not the whole array of the peptides but only few representative members that can be considered as a basis (or a set of reference points) for characterization of the structure−activity relationships (SARs) of L-AMP.

The latarcin family of L-AMP, isolated from the venom of the *Lachesana tarabaevi* spider (*13*) consists of a number of peptides with a wide spectrum of antibacterial activity and represents a suitable model for SAR investigation. We have previously characterized the Ltc2a peptide, the most active latarcin, using a combination of experimental and simulation techniques (*14*). According to our findings, this peptide in the membrane environment is featured by helix−hinge−helix structure and disturbs the phospholipid organization of the membrane via the carpet mechanism. Further analysis of the sequences of the latarcins, along with their activities toward model membranes and bacterial cells, has revealed quite a unique member of the family, the Ltc1 peptide. Its antimicrobial properties are similar to those of Ltc2a (*13*). The both peptides have the same length (26 amino acids) and net charge (+10). However, they differ significantly in amino acid composition, in particular, in the number of helix-breaking residues (Gly and Pro). In contrast to Ltc2a, Ltc1 does not disrupt planar bilayers formed of phospatidylethanolamine (PE) and phosphatidylglycerol (PG) (7:3 molar ratio) (*13*). This lipid composition resembles one of the inner membranes of the Gram-negative bacteria (*15*).

A range of biophysical techniques, such as solid-state nuclear magnetic resonance (NMR) spectroscopy (on ^{31}P and ^{15}N nuclei), fluorescence spectroscopy (with fluorescent dyes of different size), and electron microscopy, are implemented to assess the mechanisms of antimicrobial peptide activity, employing either model phospholipid membranes or live bacteria (*2*). New tools, e.g., atomic force microscopy imaging of surface-confined membranes and membrane-peptide systems, allowing to visualize directly peptide effects on the membranes are developing rapidly (*16–18*). In this study, we employed the previously described approach (*14*) to characterize the spatial structure of Ltc1 and its membrane perturbation mechanism. The behavior of this peptide in model membranes suggests that Ltc1 acts via a mechanism, which is different from that of Ltc2a. Also several previously described peptides, structurally related to Ltc1, were identified via a homology search in antimicrobial peptide databases. These peptides are reported to interact with the membranes similarly to Ltc1, thus providing an insight into the interrelationship between the structural organization of the peptide and its antibacterial action.

MATERIALS AND METHODS

Materials. The phospholipids used in the work, dioleoylphosphatidylethanolamine (DOPE) and dioleoylphosphatidylglycerol (DOPG), as well as polycarbonate membranes of 100 or 400 nm pore diameter were obtained from Avanti Polar Lipids (Alabaster, AL). Carboxyfluorescein (CBF), sodium dodecyl sulfate (SDS), and Sephadex G-50 were products of Sigma-Aldrich (St Louis, MO). Deuterated SDS (SDS-d_{25}) was a product of Cambridge Isotope Laboratories (Andover, MA). ^2H_2O (99.9%) was purchased from ISOTOPE (Russian Federation).

Sample Preparation. Ltc1 was synthesized by Fmoc methodology and purified by reverse-phase HPLC. The purity of the peptide (>95%) was checked by reverse-phase high-performance liquid chromatography (HPLC) and matrix-assisted laser desorption ionization (MALDI) mass spectrometry. A sample for the study of Ltc1 in SDS micellar solution was obtained by stepwise addition of SDS to an aqueous solution of the peptide. Chemical shifts of the peptide protons were monitored during titration. The proton signals went to their plateau values at a SDS/peptide molar ratio of ~40:1. An additional portion of SDS was added (to reach the ratio of 60:1), to make the conditions comparable to those used in the study of Ltc2a peptide (*14*). For this sample, which contained 3.1 mg of the peptide and 19.0 mg of SDS-d_{25} dissolved in 500 μL of $H_2O/^2H_2O$ (9:1, v/v) mixture (60:1 SDS-d_{25}/Ltc1 at pH 7.0), a full set of ^1H NMR spectra for structural characterization of the peptide, 2D nuclear Overhauser effect spectroscopy (NOESY, mixing time of 60–250 ms), and 2D total correlation spectroscopy (TOCSY, mixing time of 40–80 ms) were measured at 40°C. After acquisition of these spectra, the sample was lyophilized and redissolved in ^2H_2O (500 μL) to measure the H−D exchange rates of the amide protons.

DOPE/DOPG (molar ratio 7:3) liposomes were prepared by mixing required amounts of the phospholipids in chloroform followed by solvent evaporation on a Savant Speedvac vacuum dryer, model SPD1010 (GMI, Inc., Albertville, MN). The lipid film obtained was dried overnight at a high vacuum and then hydrated with 50 mM Tris-HCl (pH 7.5) and 100 mM KCl buffer prepared in $H_2O/^2H_2O$ (50:50, v/v). Freeze−thawing was used to facilitate the film soaking. The phospholipid dispersion was extruded through a polycarbonate filter with a pore size of 400 nm. Freshly prepared and size-calibrated unilamellar vesicles (LUVs) in the buffer (total lipid of 6 mg/240 μL) were placed in a NMR tube with an outer diameter of 5 mm. The peptide dissolved in the same buffer was added to the liposomes in 5 μL portions, and the tube was shaken to facilitate sample homogenization.

Homology Search. A set of short L-AMP sequences (15–40 amino acids) was derived from the Swiss-Prot (http://cn.expasy.org/sprot/) and APD databases (http://aps.unmc.edu/AP/main.php). Sequence analysis was performed using home-developed auxiliary programs. The following properties were considered: the lengths of sequence fragments uninterrupted by Gly or Pro, their charges, helicity, hydrophobicity, and hydrophobic moments. Identification of the putative helical fragments in the peptides was performed using criteria of helix propagation and N-cap propensities of the amino acids in 40 vol % trifluoroethanol (TFE) (*19*). Hydrophobic characteristics were estimated according to the White and Wimley scale (*20*).

Circular Dichroism (CD) Spectroscopy. CD spectra were measured on a JASCO-810 spectropolarimeter. All of the spectra were obtained at room temperature with quartz cells of 0.1 or 0.5 mm path length. The peptide concentration varied from ~7 μM to 1.1 mM. The spectra were baseline-corrected and then smoothed, and the helical content was estimated as previously described (*21*).

NMR Spectroscopy. ^1H and ^{31}P NMR spectra were measured on a Bruker Avance DRX 500 spectrometer (Bruker, Germany). The details of measurements and data processing were similar to those reported earlier (*14*). For

the line-shape simulation of ^{31}P NMR spectra, the program P-FIT was used. It was assumed that the lines were purely Lorentzian and the liposomes adopted an ellipsoidal shape in the magnetic field (*22*). The adjustable parameters in the simulation protocol were the components of the tensor of chemical-shift anisotropy (CSA), the integral intensity, the semiaxis ratio of the ellipsoid, and the half-width of the Lorentzian band.

Spatial Structure Calculation and Analysis. The spatial structure of Ltc1 bound to SDS micelle was calculated using CYANA (*23*), as was described (*14*). A total of 20 structures from 200 calculated with lowest violations of NMR constraints were selected. The Monte Carlo (MC) simulations were performed to get rid of the conformations falling into unfavorable regions of the Ramachandran map, according to the protocol described earlier (*14*). Visualization and analysis of the calculated structures were achieved with the MOLMOL (version 2.2) (*24*) and PROCHECK (version 3.4.4.) software (*25, 26*).

Molecular Modeling. The details of the implicit membrane model are given elsewhere (*27*). Briefly, the membrane was represented by an effective potential based on a combined employment of atomic solvation parameters for gas to octanol and gas to water transfer. The conformational space of proteins was explored via a variable-temperature MC search in the torsion angles space using the modified FANTOM program (*28*). The starting structures were arbitrarily placed in the aqueous phase. Then, several consecutive MC runs for each starting conformation with applied NMR restraints were carried out.

Hydrophobic properties of α helices were calculated and visualized using the molecular hydrophobicity potential (MHP) approach as described elsewhere (*29*).

Leakage Experiments. DOPE/DOPG (7:3) lipid film was hydrated with 50 mM Tris-HCl and 100 mM KCl at pH 7.5 buffer containing 50 mM CBF. The lipid dispersions were freeze−thawed and extruded through a polycarbonate filter with a pore size of 100 nm. Nontrapped CBF was removed by gel filtration on a Sephadex G-50 column equilibrated with the CBF-free buffer. The vesicles were then diluted to a final volume of 1.2 mL (lipid concentration of ∼20 μM), and the release of CBF upon the addition of the peptide was monitored by measuring the fluorescence intensity at 515 nm with excitation at 492 nm on a Hitachi F-4000 instrument at room temperature. The release of CBF was calculated according to the equation

$$R_f = 100[(F_t - F_0)/(F_{100} - F_0)]$$

where R_f is the percentage of the dye released and F_0, F_t, and F_{100} are the fluorescence intensities at time points $t = 0$ (i.e., prior to the peptide addition), t (∼2 min after the peptide addition accompanied by sample stirring), or after the addition of 10 μL of 10% Triton X-100 solution, respectively.

Experiments on Planar Membranes. The peptide was tested for its ability to cause conductance changes in planar bilayer membranes. The bilayers were prepared according to the Mueller−Rudin technique (*30*). The apparatus consisted of two Teflon compartments, 2 mL volume each. Membranes were made of the mixture of dioleoylphosphatidylethanolamine (DOPE) and dioleoylphosphatidylglycerol (DOPG) (7:3, mol/mol) dissolved in decane (20 mg/mL). For electrical measurements, the planar membranes were voltage-clamped via a pair of Ag/AgCl electrodes. All of the measurements were performed at room temperature with a bathing solution of 100 mM KCl in 10 mM HEPES (pH 7.0) buffer. The peptide was dissolved in distilled water (1 mg/mL) and added to the upper (*cis*) compartment. The opposite, *trans* compartment was held at ground, whereas the *cis* chamber was clamped at holding potentials relative to the ground. The current through the membrane was measured with an Axopatch 200B amplifier (Axon Instruments) and digitized with an L-780 ADC (L-card, Russia). The voltage across the membrane was clamped at 20 mV for 10 min to attain a steady-state distribution of the peptide between the membrane and the buffer. Then, the voltage amplitude was raised, starting from 20 mV, in 10 mV steps, with alternating polarity switching at each step (i.e., 20, −20, 30, −30, etc.) until −100 mV was reached. The duration of each step lasted for 30 s. Different peptide concentrations, starting from 10 nM, were tested.

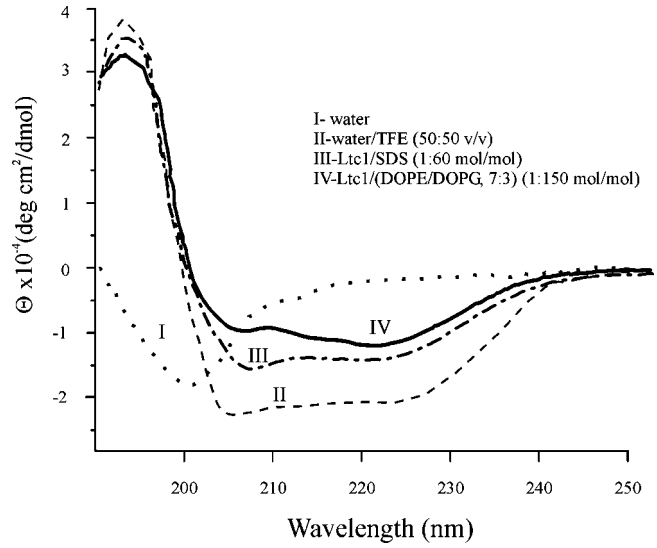

FIGURE 1: CD spectra of Ltc1 in various environments at 18 °C and pH 7.0: (I) 1.1 mM in water (• • •), (II) 0.55 mM in water/TFE (50:50, v/v) (- - -), (III) 0.45 mM in SDS micelles (60:1 SDS/peptide) (- • -), and (IV) 7.3 μM in DOPE/DOPG (7:3) LUV (diameter of 100 nm), 150:1 L/P (—).

RESULTS

Choice of Membrane-like Environment for Structural Study. To choose an appropriate environment for NMR experiments, the secondary structure of Ltc1 was investigated in aqueous solution and different membrane-like environments by CD spectroscopy. Water/TFE mixture, SDS micelles, and phospholipid liposomes were used as membrane mimics. The phospholipid liposomes composed of the DOPE/DOPG (molar ratio 7:3) mixture were chosen to imitate the phospholipid composition of the inner membrane of Gram-negative bacteria (*15*). The CD spectrum of Ltc1 in water shows a random coil structure (Figure 1). In membrane-like environments, the peptide forms a helical structure according to the CD data (Figure 1). The helical contents were estimated to be 65, 45, and 40% for water/TFE, SDS micelles, and DOPE/DOPG (7:3) LUV, respectively. The helical content in SDS micelles is similar to that in the liposomes. Therefore, an appropriate medium for high-

FIGURE 2: Summary of NOE connectivities from NOESY spectrum (mixing time of 60 ms) of Ltc1/SDS-d_{25} (1:60) at pH 7.0 and 45 °C, the CαH chemical-shift indices, and amide proton H−D exchange rates. The widths of the bars are proportional to the relative volume of the corresponding cross-peaks in the NOESY spectrum. The filled triangles and circles correspond to the amides after ~7 and 3.5 h of the H−D exchange, respectively. The volumes of overlapped cross-peaks under the chosen conditions were evaluated from NOESY spectra measured at slightly different temperatures.

Table 1: Structural Statistics for the Final Family of 20 Ltc1 Structures[a]

parameter	value
target function (Å)	0.11 ± 0.00
upper limit violations (Å)	
sum	0.8 ± 0.0
maximum	0.18 ± 0.00
lower limit violations (Å)	
sum	0.0 ± 0.0
maximum	0.00 ± 0.00
van der Waals violations (Å)	
sum	0.0 ± 0.0
maximum	0.01 ± 0.00
violations of torsion angle constraints (deg)	
sum	0.0 ± 0.0
maximum	0.00 ± 0.00
pairwise rmsd (Å)	
backbone, residues 8–23	0.44 ± 0.16(0.29 ± 0.22)
heavy atoms, residues 8–23	1.87 ± 0.26(1.21 ± 0.35)
Ramachandran statistics[b]	
residues in most favored regions (%)	78.6 (89.5)
residues in additionally allowed regions (%)	15.9 (10.0)
residues in generously allowed regions (%)	2.7 (0.5)
residues in disallowed regions (%)	2.7 (0)

[a] The values were obtained via calculations with constraints generated from 60 ms NOESY spectrum. Those after restrained minimization are given in parentheses. [b] Analyzed using PROCHECK, version 3.4.4 (*25, 26*).

resolution NMR spectroscopy, SDS micelles, were used for the determination of the spatial structure of Ltc1.

Spatial Structure. The NOESY ^{1}H NMR spectrum of Ltc1 in SDS micelles exhibits a number of strong d_{NN}, $d_{\alpha N}$ (i, i + 3), $d_{\alpha\beta}$ (i, i + 3), $d_{\alpha N}$ (i, i + 4) NOE connectivities shown in Figure 2. These connectivities, which are typical for an α-helical structure, extend from 8 to 23 residues without interruption, indicating that the peptide forms a continuous α helix in this region (Figure 2). As many as 146 distance and 127 torsion angle constraints were obtained from the NMR data for the spatial structure determination. Finally, the set of 20 structures with improved Ramachandran statistics (Table 1) was obtained via the MC refinement. Figure 3a shows these 20 structures of Ltc1. As seen from Figure 3a, the peptide helix (residues 8–23) is well-defined with the pairwise backbone root-mean-square deviation (rmsd) of 0.29 ± 0.22 Å. In contrast, both termini of the

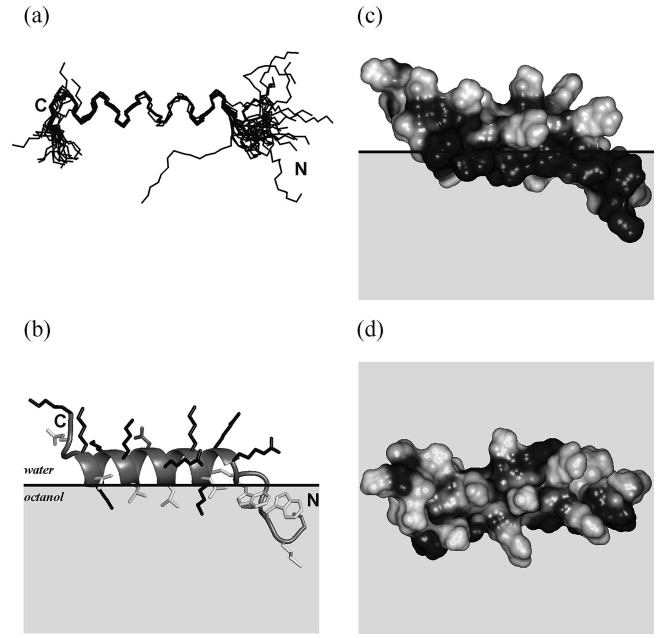

FIGURE 3: Structure of Ltc1 in SDS micelle based on the CYANA structure calculation from NMR data followed by restrained MC simulations in the implicit membrane. Ensemble of 20 representative structures superimposed by backbone atoms of residues 8–23 (a). Positioning of the best structure on the water-octanol slab (b). The peptide backbone is given as a ribbon representation. Charged, polar, and hydrophobic residues are shown by black, dark, and light gray sticks, respectively. Spatial hydrophobic properties of the peptide surface: side (c) and top (d) views. The peptide surface is colored according to the values of the molecular hydrophobicity potential (MHP) created on the surface by the Ltc1 atoms. Hydrophobic (high MHP) and hydrophilic (low MHP) surface regions are shown in dark and light gray, respectively.

peptide are poorly structured (Figure 3a). Overall, the peptide has the following hydrophobic/hydrophilic organization: an unordered comparatively hydrophobic N-terminal fragment, a prominent amphiphilic α helix, and a short hydrophilic C-terminal region. The localization of the peptide molecule in the implicit membrane and the spatial arrangement of its hydrophobic/hydrophilic domains are shown in parts b−d of Figure 3. The peptide helix lies nearly parallel to the slab with the apolar Leu residues (11, 14, 18, and 22) buried into the octanol phase. The unstructured N and C termini of the molecule are located within the octanol and water phases, respectively.

To obtain insight into the mechanism of antimicrobial activity of Ltc1, we investigated its effect on model membranes.

Interaction with Liposomes. The effect of the peptide on the phospholipid organization was studied by a ^{31}P NMR spectroscopy and dye-leakage measurements. The latter experiments showed that Ltc1 does not induce any release of CBF from the liposomes, even at rather high concentrations (Figure 4). Interestingly, another spider antimicrobial peptide Ltc2a (*14*) induces a significant release of the dye at the same concentrations. Effect of the both peptides on the dye release is shown in Figure 4.

A membrane perturbation effect for Ltc1 was investigated by ^{31}P NMR spectroscopy. The unilamellar PE/PG (7:3) liposomes with the diameter of 400 nm were used to facilitate homogeneous distribution of the peptide over the lipid surface. The ^{31}P NMR spectrum of these liposomes exhibits

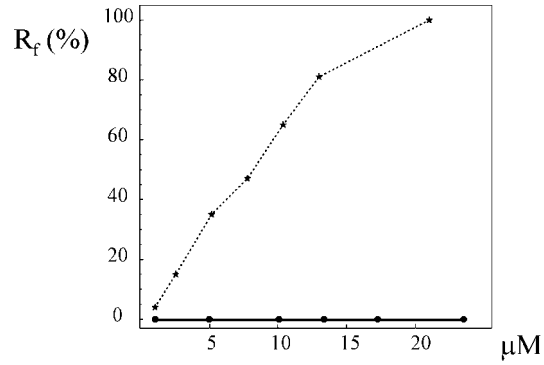

FIGURE 4: CBF release from DOPE/DOPG (7:3) LUVs (diameter of 100 nm) at pH 7.5 as a function of the Ltc1 peptide concentration. The respective data for Ltc2a peptide are shown in a dotted line.

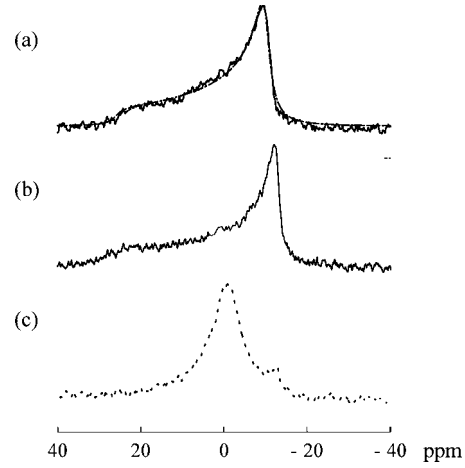

FIGURE 5: ^{31}P NMR spectra of DOPE/DOPG (7:3) liposomes (diameter of 400 nm) in the absence (a) or presence (b) of Ltc1 at L/P of 20:1. The spectrum in (c) corresponds to one obtained in the presence of Ltc2a peptide (20:1 L/P) (*14*). The thin line in (a) corresponds to the computer-simulated spectrum obtained using the P-FIT program (*25*). The best-fit parameters of the fitting for the (a) and (b) spectra, were, respectively, the CSA value of ~36.2 and 39.8 ppm (a single axially symmetric powder pattern was assumed). An ellipsoid shape of the liposomes with the aspect ratio of $c/a \sim 1.15$, where c and a are the lengths of the axes of the ellipsoid, was found for both spectra.

a typical bilayer line shape pattern in the absence and also in the presence of Ltc1, up to the L/P of 20:1 (parts a and b of Figure 5). For a comparison, Figure 5c shows the ^{31}P NMR spectrum of the liposomes in the presence of Ltc2a (*14*), exhibiting a loss of bilayer phospholipid organization.

Effect on the Planar Membrane. Ltc1 was found to induce current fluctuations through planar membranes of the same lipid composition as in the liposome study, PE/PG (7:3). The fluctuations were detected for the peptide concentrations only above 0.6 μM and a positive potential applied (Figure 6). The sign of the potential coincides with that of the transmembrane potential in the *Escherichia coli* inner membrane. A continuous increase in the current was observed for the potentials above ~50 mV (Figure 6). Interestingly, the application of a negative potential, opposite in sign to the *E. coli* transmembrane potential switched the membrane to a nonconductive state. The subsequent reversal of the potential restored the current (Figure 6). The conductance increased without membrane rupture until the voltage of ~90 mV. At the peptide concentrations above 0.6 μM, a

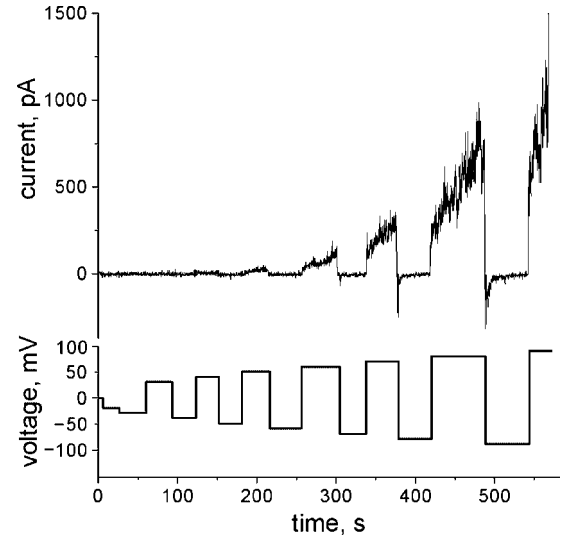

FIGURE 6: Effect of Ltc1 in planar lipid membranes composed of a DOPE/DOPG (7:3) mixture. Typical electrical activities at the peptide concentration of 0.835 μM are shown.

similar conductance pattern with higher conductance levels was observed (data not shown).

The Ltc2a peptide induced membrane breakdown at the conditions described above for the Ltc1 peptide even with no potential applied (*13*).

Homology Search and Comparison with Other Latarcins. To identify L-AMP with a sequence organization similar to Ltc1, a search was performed within the APD database (http://aps.unmc.edu/AP/main.php) and an extra set of as many as 508 peptides from Swiss-Prot. The search was confined to short sequences (15–40 amino acids) with a propensity to form a helix lacking the helix-breaking residues (Gly and Pro) and bearing a high positive net charge. This search revealed as many as 62 L-AMP with rigid helical fragments, longer than 12 amino acids. Finally, taking into account the specific properties of these fragments, such as overall length, net charge, hydrophobicity, and hydrophobic moment, only six sequences were selected (upper half of Table 2). The peptides found belong mainly to the mammalian cathelicidin family. The analysis of the sequences of other latarcins possessing antimicrobial activity (*13*) was performed in a similar way, and the results are given in the lower half of Table 2.

DISCUSSION

A key to SAR studies of antimicrobial peptides is the determination of their spatial structure in a membrane-mimicking environment. Nonpolar solvents and detergent micelles are widely used for this purpose when high-resolution NMR techniques are employed (*31*). Because differences are often found between peptide conformations in these media, a preference is often given to micelles. This was also the case in the present study, where, relying on CD spectroscopy (Figure 1), we made this choice. SDS micelles were shown to be a reasonable alternative to negatively charged membranes (*32*). At the same time, these micelles are featured by a high degree of surface curvature, and helices adsorbed to such surfaces are found to be curved (*33*). However, this was not observed in this work, because Ltc1 was found to possess a rod-like helical structure in SDS

Table 2: Characteristics of L-AMP, Homologous to Ltc1, and Other Latarcins

name (SWP)[a]	sequence[b]	L^c	Q	$\langle H \rangle$	M
	Ltc1 and Homologous Peptides				
Ltc1 (Q1ELT9)	SMWSG**MWRRKLKKLRNALKKKLK**GE	25	10	−0.59	0.38
PMAP-36 (P49931)	VG**RFRRLRKKTRKRLKKI**GKVLKWIPPIVGSIPLGCG	37	11	−0.87	0.38
BMAP-27 (P54228)	G**RFKRFRKKFKKLFKKLS**PVIPLLHLG	27	10	−0.57	0.44
CAP18 (P25230)	G**LRKRLRKFRNKIKEKLKKI**GQKIQGFVPKLAPRTDY	37	10	−0.65	0.38
plantaricin A (P80214)	AYSLQMGA**TAIKQVKKLFKKW**GW	23	5	−0.22	0.43
oxyopinin-2d (P83251)	G**KFSVFSKILRSIAKVFK**GVGKVRKQFKTASDLDKNQ	37	5	−0.11	0.40
spinigerin (P82357)	**HVDKKVADKVLLLKQLRIMRLLTR**L	25	5	−0.27	0.13
	Other Latarcins				
Ltc2a (Q1ELU1)	GLFGKLIKKFG**RKAISYAVKKAR**GKH	26	5	−0.42	0.39
Ltc3a (Q1ELU3)	**SWKSMAKKLKEYMEKLKQRA**	20	5	−0.42	0.31
Ltc3b (Q1ELU2)	**SWASMAKKLKEYMEKLKQRA**	20	4	−0.35	0.29
Ltc4a (Q1ELU5)	SLKDKVKSMG**EKLKQYIQTWKAKF**	24	3	−0.29	0.26
Ltc4b (Q1ELU4)	GLKDKFKSMG**EKLKQYIQTWKAKF**	24	3	−0.29	0.26
Ltc5 (Q1ELU9)	GFFGKMKEYFKKFGA**SFKRRFANLKKRL**	28	6	−0.48	0.34

[a] Swiss-Prot ID. [b] Predicted (see the Materials and Methods) helical fragments are bold. [c] Annotation of columns: L, total peptide length; Q, net charge of the marked helical fragment; and $\langle H \rangle$ and M, average hydrophobicity and hydrophobic moment of the fragment (*20*), respectively.

micelles. Therefore, it may be assumed that the spatial structure of Ltc1 might be the same when the peptide is bound to planar negatively charged membranes. To take into account a possible influnce of PE on the peptide structure in the PE/PG membranes, we performed long-term molecular dynamics (MD) simulations of Ltc1 in SDS micelles and full atomic models of the PE/PG (7:3) membrane (*34*). Suprisingly, the spatial structure of the peptide was found to be quiet similar in these environments. This allowed us to simplify the environment further, reducing it to implicit water−octanol slab. A mode of Ltc1 nteraction with the slab and orientation of the side chains were delineated using MC calculations using NMR restraints. This approach reveals that the Ltc1 peptide forms an uninterrupted straight amphiphilic helix in the membrane. Analysis of the two-dimensional (2D) MHP map (Figure 7) shows that the hydrophobic surface of this helix is narrow-shaped and extends along the helical axis. The rest of the surface is formed by uniformly distributed basic residues (Arg or Lys). Thus, Ltc1 significantly differs from another latarcin, Ltc2a (*14*), which has a helix−hinge−helix motif in the structure with a hydrophobicity gradient.

The effect of the both latarcins on model membranes is different too, indicating that the mechanisms of membrane perturbation exploited by these peptides are different. Indeed, in contrast to Ltc2a, which acts via the carpet mechanism (*14*), Ltc1 does not induce the release of a fluorescent marker from the DOPE/DOPG (7:3) liposomes (Figure 4). The ^{31}P NMR spectra of the PE/PG liposomes in the presence of Ltc2 and Ltc1 peptides provide evidence that only Ltc2a induces deterioration of the bilayers with the formation of an isotropic phase, while Ltc1 does not. At the same time, Ltc1 provokes fluctuations of current through planar PE/PG membranes. This effect is only observed upon application of a transmembrane potential of the same sign, as in bacteria (negative inside). The bilayer conductivity increases as a function of time and the value of the potential applied. Reversal of the potential sign ceases the membrane current with the membrane switching to a nonconductive state, indicating that the barrier function of the bilayer is restored. This means that Ltc1 does not disrupt the bilayers, which is again in line with the ^{31}P NMR data.

Ltc1 has a number of structural homologues and also helical peptides (Table 2). Their characteristic feature is the presence of a narrow hydrophobic pattern on the helix and its rigidity because of the absence of helix-breaking residues. Therefore, such helices could have a tendency to adopt an orientation parallel to the membrane plane. Indeed, this is observed in MC simulations of Ltc1 peptide as the lowest energy state in an implicit membrane (Figure 3b). This type of binding differs from typical tilted insertion exhibited by other antimicrobial peptides with a hydrophobicity gradient along the helical axis, such as Ltc2a peptide (*14*). It can be expected that peptides with a similar spatial structure effect membranes similarly. Logically, the Ltc1 homologues belonging to cathelicidins (e.g., CAP18 and its homologues from hagfish, HFIAPs, etc.) demonstrate current−voltage characteristics (*35–37*) that are similar to those of Ltc1. This effect was ascribed to the formation of variable-sized lesions (*35*), but not discrete and reproducible conductive states observed for typical ion channels or toroidal pores (e.g., alamethicin and colicin) (*38, 39*).

On the basis of our results, the following model of the Ltc1 action on Gram-negative bacteria can be proposed. The inner membrane of these bacteria has a negative surface charge. This facilitates interaction of the positively charged Ltc1 with it. Upon binding, the peptide forms amphipathic helix intercalating into the lipid matrix, lying parallel to the membrane plane. Gram-negative bacteria have a transmembrane potential, which is negative inside (*40*). This potential drives the positively charged N terminus somewhat inside of the membrane. This motion is facilitated by a relatively hydrophobic nature of Ltc1 and a helix dipole effect, originated because of the natural alignment of the amide groups with hydrogen-bonded carbonyl groups in the helix (*41*). As a result, the peptide helix adopts, most likely, transmembrane orientation. The peptide molecules form variable-sized lesions, ultimately destroying the barrier properties of the bilayer. In line with this model is the observation that Ltc1 has a moderate hemolytic activity, exhibiting hemolytic effect at the concentrations higher by at least one order of the magnitude compared to Ltc2a (*13*). This can be explained by a significantly lower transmembrane potential in erythrocytes (*42*) than in bacteria.

The mechanism described is also supported by the following obseravtions. The CAP18 peptide and its analogue shortend by the 12 C-terminal residues (rCAP18$_{106–137}$ and

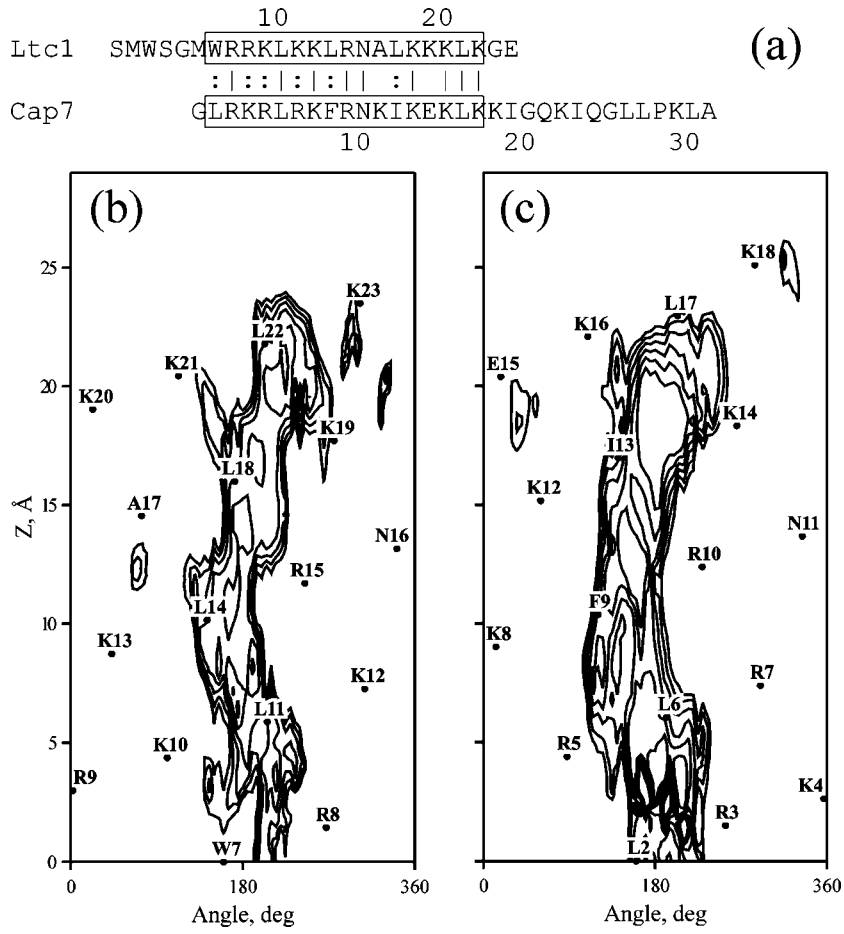

FIGURE 7: Sequence alignment between Ltc1 and structurally similar L-AMP (a) and hydrophobic organization of Ltc1 (b) and CAP18 (c). Identical and isofunctional amino acids in the alignment are marked with the symbols "|" and ":", respectively. The helical regions of the peptides are enclosed in boxes. The molecular hydrophobicity potential (MHP) on the surface of the peptide helices (b−c) corresponds to octanol−water log *P* units. The value of the rotation angle about the axis of the helix and the distance along it are plotted on the *x* and *y* axes, respectively. Only the hydrophobic areas with MHP > 0.09 are shown. Contour intervals are 0.015. The residue positions are indicated by letters and numbers. The CAP18 coordinates available in the Protein Data Bank under accession code 1LYP were used for the MHP plot in (c).

rCAP18$_{106–125}$ peptides, respectively) were shown to exhibit similar electrical activity (*36*). The Ltc1 peptide is helical in the region of 8–23 residues, and this region is one of the homology between all of these peptides (Figure 7). This implies that this peptide fragment, the 16-residue helix, is responsible for the membrane effects of these peptides. Thus, in contrast to the typical helix−hinge−helix Ltc2a peptide (*14*), Ltc1 does not interact with the membrane in a carpet manner. On the basis of high similarity of Ltc1 and several mammalian cathelicidins in their 3D structure/hydrophobicity characteristics (single rigid helix with a high positive charge and extended narrow hydrophobic pattern on the peptide surface) (Table 2) and their behavior in model membranes (*37–39*), we conclude that a membrane-potential-dependent mode of action is specific for the peptides of this type. It is necessary to stress that this mode of action is different from one of magainins, pore-forming peptides (*43*). Incorporation of PE was found to inhibit the magainin-induced pore formation, suggesting that the peptide imposes positive curvature strain, facilitating the formation of a torus-type pore, and that the presence of negative curvature-inducing lipids, such as PE, inhibits pore formation (*44*). The Ltc1-like peptides act in the PE-containing membranes in the presence of the potential.

A question arises: whether the structural/hydrophobic properties of Ltc1 are unique or not among the latarcin family? To check this, we performed an analysis of the amino acid sequences of several latarcins characterized earlier (*13*). As seen in the lower half of Table 2, most of them (Ltc3a and Ltc3b) contain the putative rigid helical fragments, the strings of at least 13 residues without helix breakers, such as Gly and Pro. Such segments are marked in bold in the sequences. Analysis of their integral hydrophobic properties, along with the charges (Table 2), shows that only Ltc1 has the specific pattern discussed above, amphiphilic and positively charged rigid helix with a thin hydrophobicity stretch on the surface. To a lesser degree, such a pattern is also inherent in the C-terminal part of the Ltc5 peptide.

While some latarcins (Ltc1, Ltc3a, and Ltc3b) consist of a single rigid helical fragment, others exhibit a helix−hinge−helix structure, e.g., Ltc2a (*14*). A helical fragment within the N-terminal part of the Ltc4a, Ltc4b, and Ltc5 peptides and a flexible hinge around the glycine residue in the middle of these peptides are likely present too. Therefore, these peptides seem to be structurally similar to Ltc2a. Because Ltc2a acts on the membranes via the carpet mechanism (*14*), it seems reasonable to assume that the Ltc4a, Ltc4b, and Ltc5 peptides share this mode of membrane perturbation.

Hence, we propose that the latarcins under study can be divided in two groups: (i) those acting via the carpet mechanism (such as Ltc2a) and (ii) those forming voltage-dependent conductivity lesions in membranes (such as Ltc1). However, the boundary between these groups is conditional, because the hydrophobic properties of the latarcins vary smoothly (Table 2). Therefore, one can speculate that such a diversity of 3D structure/hydrophobicity charactersistics determines a wide variety of biological activities of latarcins. This results in efficient defense against a wide variety of microorganisms.

ACKNOWLEDGMENT

Access to computational facilities of the Joint Supercomputer Center (Moscow, Russia) is gratefully acknowledged.

SUPPORTING INFORMATION AVAILABLE

Figure representing the fragment of the NOESY spectrum of Ltc1 peptide in SDS micelles illustrating sequential assignments (Figure S1), figure representing deviations of α-proton chemical shifts of Ltc1 in the micelle from those in the random coiled state (Figure S2), plot of the distribution of distance constraints as a function of the residue number difference or residue number (Figure S3), and intervals of variation of dihedral angles for the set of structures, calculated using the NMR constraints (Figure S4). This material is available free of charge via the Internet at http://pubs.acs.org.

REFERENCES

1. Yeaman, M. R., and Yount, N. Y. (2007) Unifying themes in host defence effector polypeptides. *Nat. Rev. Microbiol. 5*, 727–740.
2. Brogden, K. A. (2005) Antimicrobial peptides: Pore formers or metabolic inhibitors in bacteria? *Nat. Rev. Microbiol. 3*, 238–250.
3. Bechinger, B. (1999) The structure, dynamics and orientation of antimicrobial peptides in membranes by multidimensional solid-state NMR spectroscopy. *Biochim. Biophys. Acta 1462*, 157–183.
4. Blondelle, S. E., and Houghten, R. A. (1992) Design of model amphipathic peptides having potent antimicrobial activities. *Biochemistry 50*, 12688–12694.
5. Gesell, J., Zasloff, M., and Opella, S. J. (1997) Two-dimensional ^{1}H NMR experiments show that the 23-residue magainin antibiotic peptide is an α-helix in dodecylphosphocholine micelles, sodium dodecylsulfate micelles, and trifluoroethanol/water solution. *J. Biomol. NMR 9*, 127–135.
6. Giangaspero, A., Sandri, L., and Tossi, A. (2001) Amphipathic α helical antimicrobial peptides. *Eur. J. Biochem. 268*, 5589–5600.
7. Glukhov, E., Stark, M., Burrows, L. L., and Deber, C. M. (2005) Basis for selectivity of cationic antimicrobial peptides for bacterial versus mammalian membranes. *J. Biol. Chem. 280*, 33960–33967.
8. Papo, N., and Shai, Y. (2005) A molecular mechanism for lipopolysaccharide protection of Gram-negative bacteria from antimicrobial peptides. *J. Biol. Chem. 280*, 10378–10387.
9. Papo, N., Oren, Z., Pag, U., Sahl, H. G., and Shai, Y. (2002) The consequence of sequence alteration of an amphipathic-helical antimicrobial peptide and its diastereomers. *J. Biol. Chem. 277*, 33913–33921.
10. Zelezetsky, I., Pacor, S., Pag, U., Papo, N., Shai, Y., Sahl, H. G., and Tossi, A. (2005) Controlled alteration of the shape and conformational stability of α-helical cell-lytic peptides: Effect on mode of action and cell specificity. *Biochem. J. 390*, 177–188.
11. Bechinger, B., and Lohner, K. (2006) Detergent-like actions of linear amphipathic cationic antimicrobial peptides. *Biochim. Biophys. Acta 1758*, 1529–1539.
12. Oren, Z., and Shai, Y. (1997) Selective lysis of bacteria but not mammalian cells by diastereomers of melittin: Structure−function study. *Biochemistry 36*, 1826–1835.
13. Kozlov, S. A., Vassilevski, A. A., Feofanov, A. V., Surovoy, A. Yu., Karpunin, D. V., and Grishin, E. V. (2006) Latarcins: Antimicrobial and cytolytic peptides from the venom of the spider *Lachesana tarabaevi* (Zodariidae) exemplify biomolecular diversity. *J. Biol. Chem. 281*, 20983–20992.
14. Dubovskii, P. V., Volynsky, P. E., Polyansky, A. A., Chupin, V. V., Efremov, R. G., and Arseniev, A. S. (2006) Spatial structure and activity mechanism of a novel spider antimicrobial peptide. *Biochemistry 45*, 10759–10767.
15. Murzyn, K., Róg, T., and Pasenkiewicz-Gierula, M. (2005) Phosphatidylethanolamine−phosphatidylglycerol bilayer as a model of the inner bacterial membrane. *Biophys. J. 88*, 1091–1103.
16. Lam, K. L., Ishitsuka, H., Cheng, Y., Chien, K., Waring, A. J., Lehrer, R. I., and Lee, K. Y. C. (2006) Mechanism of supported membrane disruption by antimicrobial peptide protegrin-1. *J. Phys. Chem. 110*, 21282–21286.
17. Mechler, A., Praporski, S., Atmuri, K., Boland, M., Separovic, F., and Martin, L. L. (2007) Specific and selective peptide−membrane interactions revealed using quartz crystal microbalance. *Biophys. J. 93*, 3907–3916.
18. Shaw, J. E., Epand, R. F., Hsu, J. C., Mo, G. C., Epand, R. M., and Yip, C. M. (2007) Cationic peptide-induced remodelling of model membranes: Direct visualization by in situ atomic force microscopy, *J. Struct. Biol.*, in press.
19. Rohl, C. A., Chakrabartty, A., and Baldwin, R. L. (1996) Helix propagation and N-cap propensities of the amino acids measured in alanine-based peptides in 40 volume percent trifluoroethanol. *Protein Sci. 5*, 2623–2637.
20. Wimley, C., and White, H. (1996) Experimentally determined hydrophobicity scale for proteins at membrane interfaces. *Nat. Struct. Biol. 10*, 842–848.
21. Dubovskii, P. V., Li, H., Takahashi, S., Arseniev, A. S., and Akasaka, K. (2000) Structure of an analog of fusion peptide from hemagglutinin. *Protein Sci. 9*, 786–798.
22. Dubinnyi, M. A., Lesovoy, D. M., Dubovskii, P. V., Chupin, V. V., and Arseniev, A. S. (2006) Modeling of ^{31}P-NMR spectra of magnetically oriented phospholipid liposomes: A new analytical solution. *Solid State Nucl. Magn. Reson. 29*, 305–311.
23. Herrmann, T., Güntert, P., and Wüthrich, K. (2002) Protein NMR structure determination with automated NOE assignment using the new software CANDID and the torsion angle dynamics algorithm DYANA. *J. Mol. Biol. 319*, 209–227.
24. Koradi, R., Billeter, M., and Wüthrich, K. (1996) MOLMOL: A program for display and analysis of macromolecular structures. *J. Mol. Graphics 14*, 51–55.
25. Morris, L. A., MacArthur, M. W., Hutchinson, E. G., and Thornton, J. M. (1992) Stereochemical quality of protein structure coordinates. *Proteins 12*, 345–364.
26. Laskowski, R. A., MacArthur, M. W., Moss, D. S., and Thornton, J. M. (1993) PROCHECK: A program to check the stereochemical quality of protein structures. *J. Appl. Crystallogr. 26*, 283–291.
27. Efremov, R. G., Nolde, D. E., Konshina, A. G., Syrtcev, N. P., and Arseniev, A. S. (2004) Peptides and proteins in membranes: What can we learn via computer simulations? *Curr. Med. Chem. 11*, 2421–2442.
28. Nolde, D. E., Arseniev, A. S., Vergoten, G., and Efremov, R. G. (1997) Atomic solvation parameters for proteins in a membrane environment. Application to transmembrane α-helices. *J. Biomol. Struct. Dyn. 15*, 1–18.
29. Efremov, R. G., Chugunov, A. O., Pyrkov, T. V., Priestle, J. P., Arseniev, A. S., and Jacoby, E. (2007) Molecular lipophilicity in protein modeling and drug design. *Curr. Med. Chem. 14*, 393–415.
30. Mueller, P., Rudin, D. O., Tien, H. T., and Wescott, W. C. (1962) Reconstitution of cell membrane structure in vitro and its transformation into an excitable system. *Nature 194*, 979–980.
31. Strandberg, E., and Ulrich, A. S. (2004) NMR methods for studying membrane-active antimicrobial peptides. *Concepts Magn. Reson. 23A*, 89–120.
32. Li, X., Li, Y., Han, H., Miller, D. W., and Wang, G. (2006) Solution structures of human LL-37 fragments and NMR-based identification of a minimal membrane-targeting antimicrobial and anticancer region. *J. Am. Chem. Soc. 128*, 5776–5785.
33. Chou, J. J., Kaufman, J. D., Stahl, S. J., Wingfield, P. T., and Bax, A. (2002) Micelle-induced curvature in a water-insoluble HIV-1 Env peptide revealed by NMR dipolar coupling measurement in stretched polyacrylamide gel. *J. Am. Chem. Soc. 124*, 2450–2451.
34. Polyansky, A. A., Volynsky, P. E., and Efremov, R. G. (2007) Computer simulations of membrane-lytic peptides: Perspectives in drug design. *J. Bioinform. Comput. Biol. 5*, 611–626.

35. Gutsmann, T., Larrick, J. W., Seydel, U., and Wiese, A. (1999) Molecular mechanisms of interaction of rabbit CAP18 with outer membranes of Gram-negative bacteria. *Biochemistry 38*, 13643–13653.
36. Gutsmann, T., Hagge, S. O., Larrick, J. W., Seydel, U., and Wiese, A. (2001) Interaction of CAP18-derived peptides with membranes made from endotoxins or phospholipids. *Biophys. J. 80*, 2935–2945.
37. Basañez, G., Shinnar, A. E., and Zimmerberg, J. (2002) Interaction of hagfish cathelicidin antimicrobial peptides with model lipid membranes. *FEBS Lett. 532*, 115–120.
38. Woolley, G. A., Biggin, P. C., Schultz, A., Lien, L., Jaikaran, D. C., Breed, J., Crowhurst, K., and Sansom, M. S. (1997) Intrinsic rectification of ion flux in alamethicin channels: Studies with an alamethicin dimer. *Biophys. J. 73*, 770–778.
39. Sobko, A. A., Kotova, E. A., Antonenko, Y. N., Zakharov, S. D., and Cramer, W. A. (2006) Lipid dependence of the channel properties of a colicin E1-lipid toroidal pore. *J. Biol. Chem. 281*, 14408–14416.
40. Efremov, R. G., Volynsky, P. E., Nolde, D. E., van Dalen, A., de Kruijff, B., and Arseniev, A. S. (2002) Monte Carlo simulations of voltage-driven translocation of a signal sequence. *FEBS Lett. 526*, 97–100.
41. Hol, W. G. J. (1985) The role of the α-helix dipole in protein function and structure. *Prog. Biophys. Mol. Biol. 45*, 145–195.
42. Gedde, M. M., and Huestis, W. H. (1997) Membrane potential and human erythrocyte shape. *Biophys. J. 72*, 1220–1233.
43. Matsuzaki, K. (1998) Magainins as paradigm for the mode of action of pore forming polypeptides. *Biochim. Biophys. Acta 1376*, 391–400.
44. Matsuzaki, K., Sugishita, K., Ishibe, N., Ueha, M., Nakata, S., Miyajima, K., and Epand, R. M. (1998) Relationship of membrane curvature to the formation of pores by magainin 2. *Biochemistry 37*, 11856–11863.

BI702203W